Research Article Vol. 12, No. 7 / July 2025 / Optica 985

OPTICA

Continuously and widely tunable semiconductor ring lasers

Johannes Fuchsberger,[1,*,†] Theodore P. Letsou,[2,3,5,†] Dmitry Kazakov,[2,4] Rolf Szedlak,[1] Federico Capasso,[2,6,†] and Benedikt Schwarz[1,2,7,†]

[1]Institute of Solid State Electronics, TU Wien, 1040 Vienna, Austria
[2]Harvard John A. Paulson School of Engineering and Applied Sciences, Harvard University, Cambridge, Massachusetts 02138, USA
[3]Department of Electrical Engineering and Computer Science, Massachusetts Institute of Technology, Cambridge, Massachusetts 02142, USA
[4]Currently at IMEC, Leuven, Belgium
[5]tletsou@g.harvard.edu
[6]capasso@seas.harvard.edu
[7]benedikt.schwarz@tuwien.ac.at
[†]These authors contributed equally to this work.
*johannes.fuchsberger@tuwien.ac.at

Received 19 February 2025; revised 10 June 2025; accepted 11 June 2025; published 9 July 2025

Tunable semiconductor lasers are indispensable for applications ranging from spectroscopy to telecommunications, yet achieving continuous, mode-hop-free tuning across broad frequency ranges in a compact, robust device remains challenging. Here, we present a ring-array quantum cascade laser (QCL) architecture that combines the single-mode, smooth tuning of distributed feedback lasers with an extended tuning range greater than 10 cm^{-1}, all within a compact chip-scale format. Our ring-array laser employs multiple small, independently addressable ring QCLs. These rings, coupled to a shared bus waveguide, have different radii, resulting in distinct lasing frequencies. This configuration enables multi-ring spectral sweeps with stable emission facilitated by unidirectional lasing. In contrast to traditional tunable lasers, our device achieves mode-hop-free tuning over broad bandwidths, is resilient under high levels of optical feedback, and supports beam combining for broadband spectral coverage, resulting in a combined tuning range of 33 cm^{-1} from three different rings. This versatile platform offers a pathway for scalable, compact spectroscopic sources, with potential applications across the mid-infrared and beyond.

https://doi.org/10.1364/OPTICA.559884

1. INTRODUCTION

Tunable lasers play a pivotal role across a wide range of applications, from spectroscopy to telecommunications. The ability to precisely adjust a laser's output wavelength is essential for precision measurements, high-resolution imaging, and efficient communication systems [1–3]. The market for tunable lasers has grown dramatically since their advent in 1966 [4], and they are now commercially available across a range of gain media and laser configurations, such as gas lasers, fiber lasers, optical parametric oscillators (OPOs), and semiconductor lasers [5–9]. Despite the extensive variety of tunable lasers, a fundamental trade-off persists between the tuning range and tuning accuracy; achieving continuous tuning over a broad frequency range remains challenging.

This limitation highlights the unique advantage of tunable semiconductor lasers, which excel in compactness, broad wavelength accessibility (spanning from the visible to the terahertz range), and high output power—often reaching watt-level emissions [10–16]. Tunable semiconductor lasers are typically designed in one of four primary configurations [17]. For brevity, we will limit our discussion to two main geometries. The first is the distributed feedback (DFB) configuration, where a periodic grating is fabricated along the laser ridge [18]. This grating provides frequency-selective optical feedback, amplifying a single wavelength in the gain medium while suppressing all others. Tunability is achieved by adjusting the laser's drive current or its temperature. The second configuration is the external cavity setup, where a rotating diffraction grating reflects a single wavelength into the laser cavity, causing it to lase. The reflected wavelength is tuned by mechanically adjusting the angle of the grating [19].

Each type of tunable semiconductor laser has its advantages and disadvantages. On the one hand, DFB lasers require complicated fabrication protocols and can only tune a small amount around their center wavelength. For example, commercially available DFB lasers can often only provide a tuning range of $\sim 3-6\ cm^{-1}$ [20]. This narrow tuning range can be compensated for by coupling multiple DFB lasers together on-chip and combining their output with free-space or integrated light multiplexers [21–23]. On the other hand, they tune without mode hops, making them excellent mid-IR sources for probing narrow absorption features, and go-to sources for telecommunication applications. External cavity

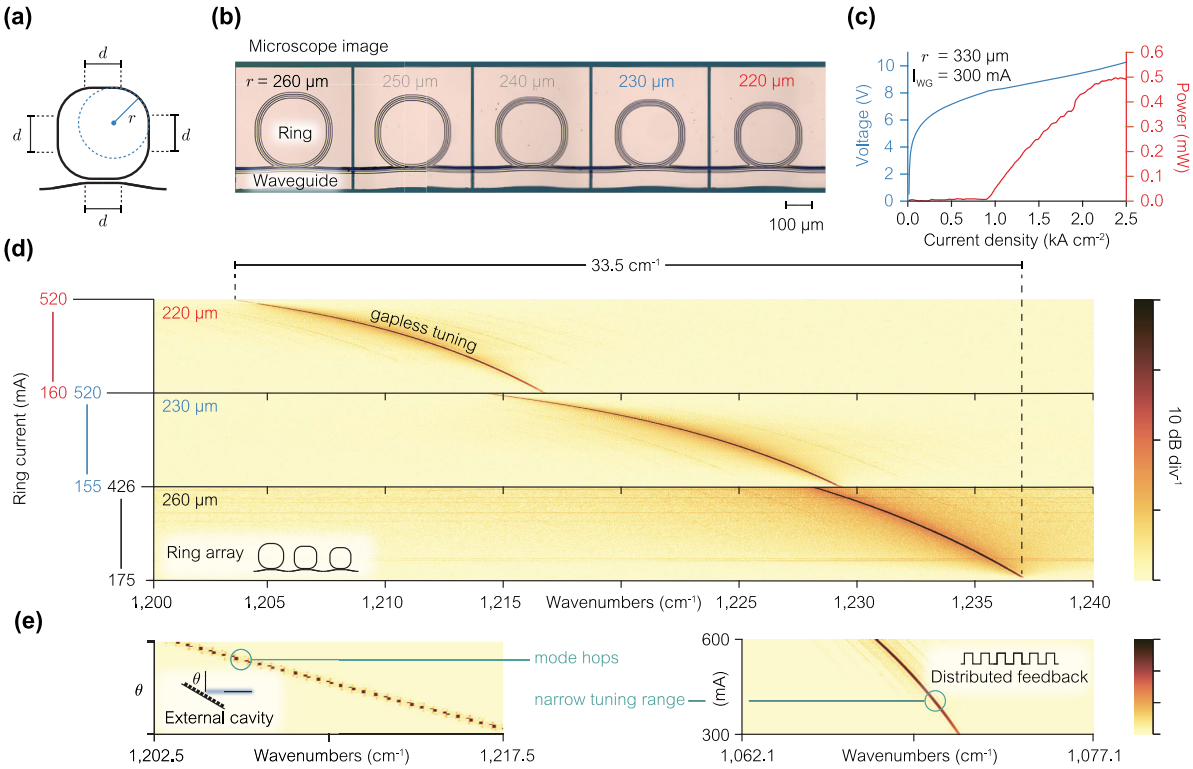

Fig. 1. Ring-array laser. (a) Shows the geometry of a single ring laser element. The laser consists of four straight sections of length d, connected by four quarter circles of radius r. Here, $d = 50$ μm and r spans from 260 to 220 μm, for this particular chip. (b) Shows a microscope image of an example ring-array laser. Each ring is connected together through a bus waveguide. The bus waveguide is separated by an air gap of 1 μm along the straight section of the ring lasers. (c) Shows a light–current–voltage (LIV) curve for an example ring with an output power exceeding 0.5 mW. (d) Three ring QCLs from a single array span over 1 THz of optical bandwidth without mode hops around a center wavelength of 8 μm. Each ring ($r = 260$, 230, and 220 μm) is tuned by increasing its bias current as shown by each y axis. This tuning is compared with that of a commercial external cavity QCL (only a small subset of the tuning range is shown) and a commercial distributed feedback (DFB) QCL in (e), both of which emit on the order of 100 mW in continuous-wave operation at room temperature. The ring-array laser displays mode hop-free tuning over three times the spectral bandwidth of the DFB QCL. Small side modes present in the spectral sweeps are a result of artifacts in the FTIR.

configurations are also difficult to fabricate but provide much larger tuning ranges compared to DFB gratings, often exceeding hundreds of cm^{-1} [24]; however, they require mechanically moving parts and are often susceptible to mode hops. The mechanical grating can be replaced by two photonic integrated double-ring mirrors acting as a Vernier feedback filter [25,26]. This allows one to achieve broad tuning ranges without the need for mechanically moving parts. Despite this, these so-called "Vernier tunable lasers" are still susceptible to mode hops.

In this work, we introduce a novel type of tunable semiconductor laser that combines the smooth tunability of the DFB laser over an extended spectral range, while preserving the chip-scale footprint and straightforward fabrication of a simple edge emitter. Our device comprises multiple small ring lasers, each with a distinct radius, all coupled to a common bus waveguide fabricated from the same quantum cascade laser (QCL) active material [27–31]. A cartoon schematic of a ring element in the ring-array laser is shown in Fig. 1(a), where r is the radius of the ring, and d is the length of the straight section connecting to the bus waveguide. Each ring has a slightly different perimeter (see Section I in Supplement 1), resulting in a unique lasing wavelength for each ring, which can be smoothly tuned over a range of 10 cm^{-1} by adjusting the laser bias. This results in a combined mode hop-free tuning range of over 33 cm^{-1} (~1 THz) over three rings in our ring-array laser. This tuning range is on par with multi-section DFB lasers without the need to fabricate a unique grating along the active region of each laser or a specially designed arrayed waveguide grating. The single-mode emission is ensured by the unidirectional operation of the ring lasers, which prevents the formation of a gain grating. Furthermore, parametric single-mode instabilities—commonly known to destabilize single-mode lasing in QCLs—are avoided by fabricating small rings with free spectral ranges (FSRs) outside the parametric gain bandwidth [32,33]. The unidirectional operation of our laser chip maintains a stable wavelength output even under intense optical injection ($P_{injected} = 75$ mW) onto the laser facet. Finally, our design is modular; ring lasers can be operated individually or simultaneously, which allows us to combine the output of several rings into one beam emitted from one facet.

2. FREQUENCY TUNING OF THE RING-ARRAY LASER

An example ring-array laser is shown in Fig. 1(b). The device comprises five ring QCLs, each with a distinct radius r ranging from 220 to 260 μm and a coupling section of 50 μm. Each ring radius satisfies the round-trip lasing condition with a unique wavelength close to the peak of the gain. This design allows us to span a large portion of the QCL gain bandwidth by changing the ring size (see Section II in Supplement 1). Our ring QCLs are fabricated using a dry-etch process and show excellent performance

with epitaxial side-up mounting on copper submounts. Separate electrical contacts are fabricated for each ring QCL and the bus waveguide. This flexibility allows us to partially reduce the optical loss of the bus waveguide, which is approximately 1.5 cm^{-1} [34], (or amplify the light emitted from the rings) through electrical bias (see Section III in Supplement 1). A single-ring QCL is capable of emitting up to 0.5 mW of optical power in continuous-wave operation at room temperature [Fig. 1(c)] when the bus waveguide is biased to 300 mA. The low-threshold QCL wafer used in this initial demonstration ($J_{th} \sim 1$ kA cm^{-2} at 8 μm) provides a wide dynamic range of bias. A typical ring tunes >10 cm^{-1} from threshold to rollover. Sequentially biasing three rings allows us to smoothly sweep >33 cm^{-1} of optical bandwidth (ring 1 : 8.87 cm^{-1} 266 GHz, ring 2 : 14.81 cm^{-1}, 444 GHz, and ring 3 : 13.16 cm^{-1}, 395 GHz) with minimal spectral overlap between each ring, only 2.89 cm^{-1}, as shown in Fig. 1(d).

For a direct comparison with commercially available QCL-based tunable lasers, we used an external cavity QCL that emits at 8 μm (DRS Daylight Solutions, ECQCL) and a DFB QCL that emits at 10 μm (Thorlabs, DFB), with all comparisons made in spectroscopic wavenumbers (cm^{-1}). Figure 1(e) shows a spectral sweep of the ECQCL and a spectral sweep of the DFB on the left and right sides of the figure, respectively. The ECQCL is capable of tuning >200 cm^{-1} around its gain peak by adjusting its grating angle (only a small subset of the full spectral sweep is shown here; the full spectral sweep can be found in the supplemental materials of [34]), but has discontinuities in spectral tuning due to mode hops. The commercial DFB QCL, on the other hand, tunes smoothly with bias current, but only over ~4 cm^{-1}. The output of a single ring in our ring-array laser can tune without mode hops over a greater spectral range than the DFB QCL. The broader tuning range of the grating-free rings is partially attributed to their lower losses compared to DFB lasers, which allow them to lase over a larger temperature range, approximately 153 K (see Section I in Supplement 1). However, we should note that state-of-the-art DFB QCLs have integrated heaters fabricated adjacent to their active cores, extending their tuning ranges to over 12 cm^{-1} [35].

The main difference between our ring-array laser and other ring QCLs is the method of light emission. Most compact ring QCLs are either surface emitting [36,37] or substrate emitting [38,39]. On the other hand, our ring-array laser is facet-emitting through a bus waveguide [27], permitting beam-combining. In addition, the ability to bias our ring-array laser in continuous-wave operation results in a stable frequency output over time [40,41]. In contrast, other demonstrations of surface-emitting ring QCLs often exhibit frequency chirping during the duration of a pulsed bias [42].

3. BEAM COMBINING

Traditional tunable lasers emit a single wavelength at a time. In contrast, the modularity of ring-array lasers enables multiple rings to operate simultaneously, with each ring having independent electrical contacts for individual or concurrent biasing. Single-facet emission of multiple laser colors is achieved by combining beams from each ring into a single bus waveguide using evanescent directional couplers along straight sections of the lasers [27]. Similar beam-combining techniques have been employed in tunable lasers to combine the outputs of multiple DFB QCLs using passive waveguides [43] or active Y-couplers [44]. The bottom three plots of Fig. 2(a) show the normalized power spectral density (PSD) measured for three different rings (190, 210, and 220 μm) under a single bias condition. As expected, each ring emits at a different wavelength due to variations in their radii. The top plot of Fig. 2(a) displays the PSD of the ring-array laser with all three

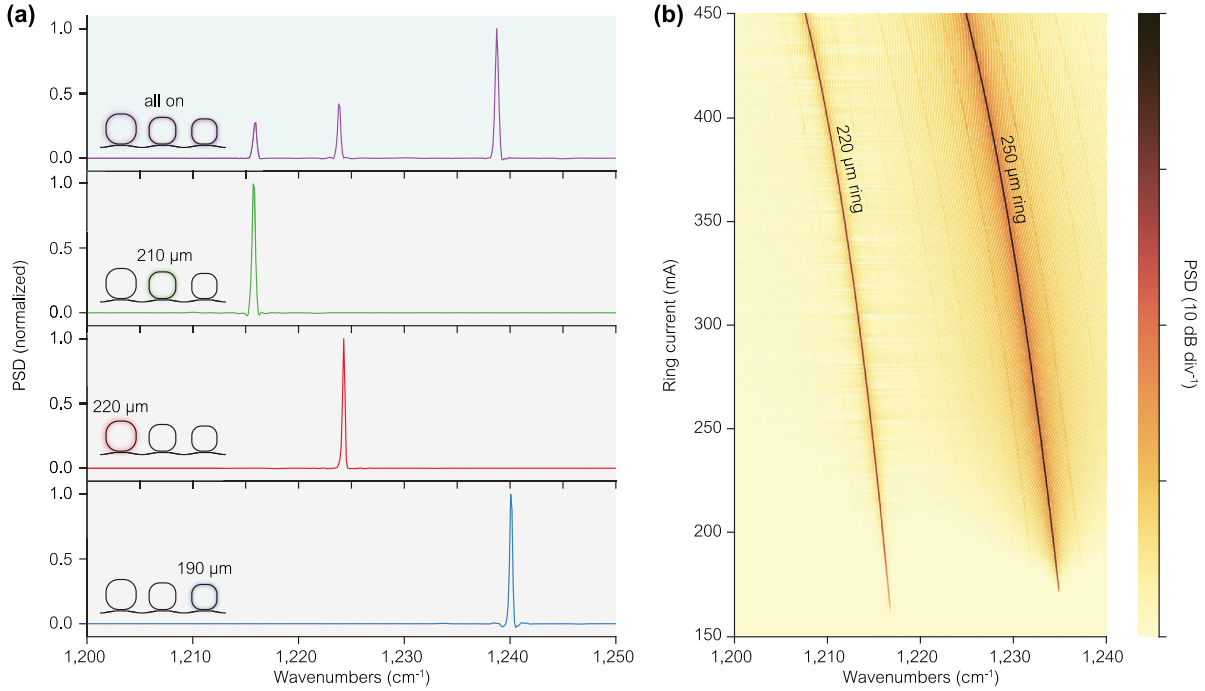

Fig. 2. Beam combining in the ring-array laser. (a) The ring-array laser can be operated either individually, with a single ring laser active at a time, or collectively, with all rings operating simultaneously. The bottom three plots show the normalized power spectral density (PSD) of three individual rings in the ring-array laser (190, 210, and 220 μm). The top plot displays the laser spectrum when all three rings are operated simultaneously, demonstrating that each ring's wavelength remains stable regardless of emission from neighboring rings. This stability enables multi-ring spectral sweeps, as shown in (b). Here, two rings (220 and 250 μm) are biased from 150 to 450 mA, causing both to sweep spectrally at the same time.

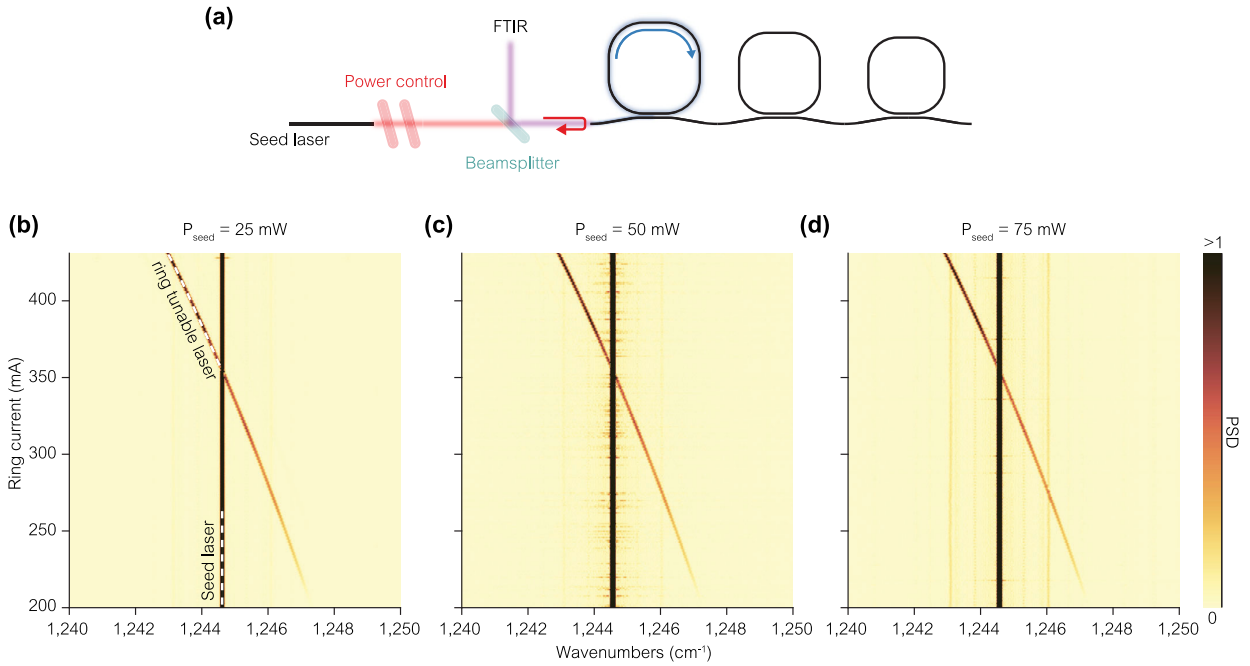

Fig. 3. Feedback-insensitive tuning of the tunable source. (a) Shows the setup used to experimentally characterize the stability of our ring-array laser. An external cavity QCL (ECQCL) serves as a powerful seed laser injected into the facet of the waveguide of the ring-array laser. The power of the seed laser is controlled by adjusting the relative orientations of a polarizer–analyzer pair. A beam splitter is used to simultaneously measure the output spectrum of the ring-array laser as a function of bias while injecting the seed laser. (b), (c), and (d) show spectral sweeps of the ring-array laser for seed injection powers of 25, 50, and 75 mW, respectively, both of which are labeled with a dashed white line. The spectral sweep of the ring-array laser remains identical regardless of seed power.

rings biased simultaneously. Although the rings lase at slightly different wavelengths, compared to individual operation because of small ring-to-ring coupling through the bus, they maintain similar spectral profiles measured from a single facet of the bus waveguide. The ability to combine the output of multiple rings into a single waveguide enables multi-ring spectral sweeps. Figure 2(b) shows a heat map of the PSD measured from two rings as their bias currents are simultaneously swept from 150 to 450 mA, from below their lasing thresholds to near their thermal rollovers. Each ring tunes $>10\,\mathrm{cm}^{-1}$ independently during the current sweep without destabilizing in the presence of emissions from the other ring. This beam-combining effect can be used to probe multiple absorption lines simultaneously—without switching the source—enabling fast, broadband spectroscopy. In particular, wavelength-modulation spectroscopy (WMS), which requires continuous tuning over a narrow absorption feature [45], stands to benefit significantly from the ring-array laser's broad, multi-color tuning. Furthermore, spectroscopy using the ring-array laser may provide an alternative to dual-comb spectroscopy, a technique commonly implemented using QCL-based frequency combs [46].

4. FEEDBACK INSENSITIVITY

A key difference between the ring-array laser presented here and other types of tunable semiconductor lasers is its unidirectional mode of operation. Tunable lasers that use Fabry–Perot bars as a gain section are inherently bidirectional, with the laser field propagating in both directions along the cavity. This bidirectional behavior significantly impacts laser emission, often resulting in a multi-mode spectral output due to the formation of a gain grating within the cavity in the absence of a frequency-selective grating. Another consequence of bidirectional behavior is an increased sensitivity to optical feedback, leading to mode destabilization and increased intensity noise in DFB lasers [47–49]. In principle, external isolators or feedback control mechanisms can suppress feedback effects to maintain stable operation; however, isolation optics are often bulky and can reduce output power in laser systems, especially in the mid-infrared spectral range where transmissive optics are less readily available compared to telecom wavelengths. In contrast, the unidirectional nature of the ring-array laser naturally mitigates feedback sensitivity, eliminating the need for feedback-control optics. Any back-reflections or external signals re-entering the cavity through the bus waveguide travel in the opposite direction of the lasing field and, therefore, do not couple to or destabilize the laser field [50].

We perform a simple injection experiment, as shown in Fig. 3(a), to demonstrate the stability of our ring-array laser under high levels of optical injection. Light from an ECQCL, referred to as the seed laser, resonant with the emission wavelength of the ring-array laser, is injected into the facet of the ring-array laser through a beam splitter. The power of the seed laser is controlled using a polarizer–analyzer pair, while we measure a spectral sweep of the ring-array laser. Back-reflected light from the seed laser off the facet of the bus waveguide enables simultaneous spectral acquisition of both the seed laser and the ring-array laser. Figures 3(b)–3(d) show heat maps of the PSD of both lasers as a function of ring current under three levels of optical injection (25, 50, and 75 mW, respectively). The ring-array laser tunes smoothly over $5\,\mathrm{cm}^{-1}$ regardless of the power of the seed laser, even when the seed laser and the ring-array laser are fully resonant with each other. Interestingly, back-reflections from the waveguide facet begin to destabilize the seed laser, as indicated by the spectral jitter in the seed laser line.

This demonstrates that the ring-array laser could be an ideal source for heterodyning, as its spectrum remains single-mode and stable under high amounts of optical injection. In stark contrast, other sources used for spectroscopy, such as QCL frequency combs based on Fabry–Perot geometries, suffer catastrophic optical feedback, collapsing their outputs to a single frequency [51].

5. CONCLUSION AND OUTLOOK

We introduced a tunable semiconductor laser source that combines broad spectral coverage (over 33 cm^{-1}) without mode hops. The ring-array laser is ideally suited for mid-infrared applications such as multi-line gas spectroscopy—for example, wavelength-modulation spectroscopy of CO_2 and CH_4—and can also support free-space links in the 3–5 μm window via wavelength-division multiplexing, all emitted from a single facet.

The ring-array laser is remarkably stable under high amounts of optical injection, tuning identically under 75 mW of resonant injection as it does under no optical injection, which makes it an excellent candidate for heterodyne or multi-heterodyne measurements. In practice, one can operate more than three rings at once—limited only by the number of low-noise current drivers and the chip's thermal management—to further extend the spectral coverage without significant additional complexity.

The integrated bus waveguide, which connects each ring in the ring-array laser, serves as both a method for beam combining and amplification, enabling facet emission of multiple laser frequencies simultaneously. Importantly, all components of our ring-array laser can be defined using a single photolithography step, without the need for a feedback grating using e-beam lithography. As a result, the ring-array laser is highly compatible with wafer-scale fabrication [52]. Furthermore, several engineering improvements can be easily implemented in the ring-array laser with little change in the fabrication protocol. Antireflective facet coatings and epi-down mounting for added thermal dissipation can lead to higher output powers, while S-shaped cross arms with Y-junctions can be utilized to enforce the lasing directionality of each ring [53]. Finally, while our initial demonstration uses a QCL active region operating at 8 μm, we believe the ring-array laser is agnostic to the center emission wavelength and even the type of the semiconductor gain medium. The ring-array laser geometry can be transferred to other semiconductor platforms, such as interband cascade lasers, quantum well lasers, and quantum dot lasers, extending the spectral coverage of the ring-array laser beyond the mid-infrared.

Funding. European Research Council (853014); National Science Foundation (ECCS-2221715).

Acknowledgment. J. Fuchsberger thanks the Marshall Plan Foundation Fellowship Program. T. P. Letsou thanks the Department of Defense (DoD) through the National Defense Science and Engineering Graduate (NDSEG) Fellowship Program. J. Fuchsberger, R. Szedlak, and B. Schwarz received funding from the European Research Council (ERC) under the European Union's Horizon 2020 research and innovation program (853014). This material is based on work supported by the National Science Foundation (100000001) (ECCS-2221715). The authors gratefully acknowledge the Center for Micro- and Nanostructures (ZMNS) of TU Wien for providing the cleanroom facilities. The authors acknowledge TU Wien Bibliothek for financial support through its Open Access Funding Programme.

Disclosures. The authors declare the existence of a financial competing interest. The Research and Transfer Support Office of TU Wien has begun the process of filing a joint patent application with Harvard University based on the materials of this work and is exploring commercialization opportunities for the presented technology.

Data availability. Data underlying the results presented in this paper are not publicly available at this time but may be obtained from the authors upon reasonable request.

Supplemental document. See Supplement 1 for supporting content.

REFERENCES

1. B. Shi, Y.-H. Luo, W. Sun, *et al.*, "Frequency-comb-linearized, widely tunable lasers for coherent ranging," Photonics Res. **12**, 663–681 (2024).
2. H. Farrokhi, T. M. Rohith, J. Boonruangkan, *et al.*, "High-brightness laser imaging with tunable speckle reduction enabled by electroactive micro-optic diffusers," Sci. Rep. **7**, 15318 (2017).
3. M. Troncoso-Costas, G. Jain, Y. Li, *et al.*, "Experimental demonstration of 480 Gbit/s coherent transmission using a nanosecond switching tuneable laser," Opt. Commun. **554**, 130164 (2024).
4. M. L. Spaeth and D. P. Bortfeld, "Stimulated emission from polymethine dyes," Appl. Phys. Lett. **9**, 179–181 (1966).
5. P. Chevalier, A. Amirzhan, F. Wang, *et al.*, "Widely tunable compact terahertz gas lasers," Science **366**, 856–860 (2019).
6. L. Ledezma, A. Roy, L. Costa, *et al.*, "Octave-spanning tunable infrared parametric oscillators in nanophotonics," Sci. Adv. **9**, eadf9711 (2023).
7. H.-J. Joo, J. Liu, M. Chen, *et al.*, "Actively tunable laser action in GeSn nanomechanical oscillators," Nat. Nanotechnol. **19**, 1116–1121 (2024).
8. M. C. Y. Huang, Y. Zhou, and C. J. Chang-Hasnain, "A nanoelectromechanical tunable laser," Nat. Photonics **2**, 180–184 (2008).
9. J. Yang, K. Van Gasse, D. M. Lukin, *et al.*, "Titanium:sapphire-on-insulator integrated lasers and amplifiers," Nature **630**, 853–859 (2024).
10. G. Zhang, M. Takiguchi, K. Tateno, *et al.*, "Telecom-band lasing in single InP/InAs heterostructure nanowires at room temperature," Sci. Adv. **5**, eaat8896 (2019).
11. B. Dong, Y. Wan, W. W. Chow, *et al.*, "Turnkey locking of quantum-dot lasers directly grown on Si," Nat. Photonics **18**, 669–676 (2024).
12. W. Jin, Q.-F. Yang, L. Chang, *et al.*, "Hertz-linewidth semiconductor lasers using CMOS-ready ultra-high-Q microresonators," Nat. Photonics **15**, 346–353 (2021).
13. S. Yamaoka, N.-P. Diamantopoulos, H. Nishi, *et al.*, "Directly modulated membrane lasers with 108 GHz bandwidth on a high-thermal-conductivity silicon carbide substrate," Nat. Photonics **15**, 28–35 (2020).
14. Y. Matsui, R. Schatz, D. Che, *et al.*, "Low-chirp isolator-free 65-GHz-bandwidth directly modulated lasers," Nat. Photonics **15**, 59–63 (2020).
15. C. A. Curwen, J. L. Reno, and B. S. Williams, "Broadband continuous single-mode tuning of a shortcavity quantum-cascade VECSEL," Nat. Photonics **13**, 855–859 (2019).
16. A. Mantz, "A review of spectroscopic applications of tunable semiconductor lasers," Spectrochim. Acta Part A **51**, 2211–2236 (1995).
17. L. Coldren, G. Fish, Y. Akulova, *et al.*, "Tunable semiconductor lasers: a tutorial," J. Lightwave Technol. **22**, 193–202 (2004).
18. J. Seufert, M. Fischer, M. Legge, *et al.*, "DFB laser diodes in the wavelength range from 760 nm to 2.5 μm," Spectrochim. Acta Part A **60**, 3243–3247 (2004).
19. B. Mroziewicz, "External cavity wavelength tunable semiconductor lasers—a review," Opto-Electron. Rev. **16**, 347–366 (2008).
20. Thorlabs, "Quantum and interband cascade lasers (QCLs and ICLs), 3–11 μm," https://www.thorlabs.com/newgrouppage9.cfm?objectgroup_id=6932, accessed 20 May 2025.
21. L. Bizet, R. Vallon, B. Parvitte, *et al.*, "Multi-gas sensing with quantum cascade laser array in the mid-infrared region," Appl. Phys. B **123**, 145 (2017).
22. T. S. Karnik, L. Diehl, Q. Du, *et al.*, "On-chip wavelength beam combined DFB quantum cascade laser arrays," Opt. Lett. **50**, 2409–2412 (2025).
23. P. Rauter and F. Capasso, "Multi-wavelength quantum cascade laser arrays," Laser Photonics Rev. **9**, 452–477 (2015).
24. Daylight Solutions, "Hedgehog™ Mid-IR Laser," https://www.daylightsolutions.com/products/hedgehog/, accessed 20 May 2025.
25. T. Komljenovic, L. Liang, R.-L. Chao, *et al.*, "Widely-tunable ring-resonator semiconductor lasers," Appl. Sci. **7**, 732 (2017).
26. J. C. Hulme, J. K. Doylend, and J. E. Bowers, "Widely tunable Vernier ring laser on hybrid silicon," Opt. Express **21**, 19718–19722 (2013).

27. D. Kazakov, T. P. Letsou, M. Beiser, *et al.*, "Active mid-infrared ring resonators," Nat. Commun. **15**, 607 (2024).
28. S. Kacmoli and C. F. Gmachl, "Quantum cascade disk and ring lasers," Appl. Phys. Lett. **124**, 010502 (2024).
29. R. Szedlak, T. Hisch, B. Schwarz, *et al.*, "Ring quantum cascade lasers with twisted wavefronts," Sci. Rep. **8**, 7998 (2018).
30. B. Meng, M. Singleton, M. Shahmohammadi, *et al.*, "Mid-infrared frequency comb from a ring quantum cascade laser," Optica **7**, 162 (2020).
31. I. Heckelmann, M. Bertrand, A. Dikopoltsev, *et al.*, "Quantum walk comb in a fast gain laser," Science **382**, 434–438 (2023).
32. M. Piccardo, B. Schwarz, D. Kazakov, *et al.*, "Frequency combs induced by phase turbulence," Nature **582**, 360–364 (2020).
33. T. S. Mansuripur, C. Vernet, P. Chevalier, *et al.*, "Single-mode instability in standing-wave lasers: the quantum cascade laser as a self-pumped parametric oscillator," Phys. Rev. A **94**, 063807 (2016).
34. D. Kazakov, T. P. Letsou, M. Piccardo, *et al.*, "Driven bright solitons on a mid-infrared laser chip," Nature **641**, 83–89 (2025).
35. A. Bismuto, Y. Bidaux, C. Tardy, *et al.*, "Extended tuning of mid-IR quantum cascade lasers using integrated resistive heaters," Opt. Express **23**, 29715–29722 (2015).
36. E. Mujagić, M. Nobile, H. Detz, *et al.*, "Ring cavity induced threshold reduction in single-mode surface emitting quantum cascade lasers," Appl. Phys. Lett. **96**, 031111 (2010).
37. A. V. Babichev, E. S. Kolodeznyi, A. G. Gladyshev, *et al.*, "Surface emitting quantum-cascade ring laser," Semiconductors **55**, 591–594 (2021).
38. Q. Guo, J. Zhang, C. Ning, *et al.*, "Continuous-wave operation of microcavity quantum cascade lasers in whispering-gallery mode," ACS Photonics **9**, 1172–1179 (2022).
39. Q. Guo, J. Zhang, R. Yin, *et al.*, "Continuous-wave microcavity quantum cascade lasers in whispering-gallery modes up to 50°C," Opt. Express **30**, 22671–22678 (2022).
40. D. H. Wu and M. Razeghi, "High power, low divergent, substrate emitting quantum cascade ring laser in continuous wave operation," APL Mater. **5**, 035505 (2017).
41. Y. Bai, S. Tsao, N. Bandyopadhyay, *et al.*, "High power, continuous wave, quantum cascade ring laser," Appl. Phys. Lett. **99**, 261104 (2011).
42. M. Brandstetter, A. Genner, C. Schwarzer, *et al.*, "Time-resolved spectral characterization of ring cavity surface emitting and ridge-type distributed feedback quantum cascade lasers by step-scan FT-IR spectroscopy," Opt. Express **22**, 2656–2664 (2014).
43. T. S. Karnik, L. Diehl, K. P. Dao, *et al.*, "Monolithic beam combined quantum cascade laser arrays with integrated arrayed waveguide gratings," Opt. Express **32**, 11681–11692 (2024).
44. W. Zhou, N. Bandyopadhyay, D. Wu, *et al.*, "Monolithically, widely tunable quantum cascade lasers based on a heterogeneous active region design," Sci. Rep. **6**, 25213 (2016).
45. A. L. Chakraborty and A. Roy, "Wavelength modulation spectroscopy," in *Modern Techniques of Spectroscopy* (Springer Singapore, 2021), pp. 321–362.
46. G. Villares, A. Hugi, S. Blaser, *et al.*, "Dual-comb spectroscopy based on quantum-cascade-laser frequency combs," Nat. Commun. **5**, 5192 (2014).
47. L. Jumpertz, M. Carras, K. Schires, *et al.*, "Regimes of external optical feedback in 5.6 μm distributed feedback mid-infrared quantum cascade lasers," Appl. Phys. Lett. **105**, 131112 (2014).
48. D. Weidmann, K. Smith, and B. Ellison, "Experimental investigation of high-frequency noise and optical feedback effects using a 97 μm continuous-wave distributed-feedback quantum-cascade laser," Appl. Opt. **46**, 947–953 (2007).
49. R. Tkach and A. Chraplyvy, "Regimes of feedback effects in 1.5-μm distributed feedback lasers," J. Lightwave Technol. **4**, 1655–1661 (1986).
50. N. Opačak, D. Kazakov, L. L. Columbo, *et al.*, "Nozaki–Bekki solitons in semiconductor lasers," Nature **625**, 685–690 (2024).
51. D. Burghoff, Y. Yang, D. J. Hayton, *et al.*, "Evaluating the coherence and time-domain profile of quantum cascade laser frequency combs," Opt. Express **23**, 1190–1202 (2015).
52. D. Stark, M. Beck, and J. Faist, "Microring quantum cascade surface emitting lasers," APL Photonics **10**, 016122 (2025).
53. C. C. Nshii, C. N. Ironside, M. Sorel, *et al.*, "A unidirectional quantum cascade ring laser," Appl. Phys. Lett. **97**, 231107 (2010).